

Supporting Information (SI)

Activity, Selectivity, and Durability of Ruthenium Nanoparticle Catalysts for Ammonia Synthesis by Reactive Molecular Dynamics Simulation: Size Effect

*Sung-Yup Kim, Hong Woo Lee, Sung Jin Pai, and Sang Soo Han**

Computational Science Research Center, Korea Institute of Science and Technology (KIST),
5 Hwarangno 14-gil, Seongbuk-gu, Seoul 02792, Republic of Korea

Corresponding Author

*sangsoo@kist.re.kr. Tel.: +82 2 958 5441. Fax: +82 2 958 5451.

S1. Details on the development of the Reactive Force Field (ReaxFF) for the Ru-N-H system

Within the framework of the reactive force field (ReaxFF), the total energy of the Ru-N-H system was expressed as follows:

$$E_{\text{System}} = E_{\text{bond}} + E_{\text{over}} + E_{\text{under}} + E_{\text{lp}} + E_{\text{val}} + E_{\text{tor}} + E_{\text{vdWaals}} + E_{\text{Coulomb}} + E_{\text{hydrogen}} \quad (\text{S1})$$

The various energy contributions in Eq. S1 include the bond energy (E_{bond}), the penalty energy for over-coordination (E_{over}), the energy to stabilize the under-coordination of atoms (E_{under}), the lone-pair energy (E_{lp}), the valence angle energy (E_{val}), the torsional energy (E_{tor}), the van der Waals energy (E_{vdWaals}), the Coulomb energy (E_{Coulomb}), and the hydrogen bond energy (E_{hydrogen}). The Coulomb energy (E_{Coulomb}) of the system was calculated using a geometry-dependent charge distribution determined using the electronegativity equalization method (EEM)^{S1}. In addition, non-bonded interactions, such as short-range Pauli repulsion and long-range dispersion, were included in the van der Waals term (E_{vdWaals}). The non-bonded interactions (E_{Coulomb} and E_{vdWaals}) were screened by a taper function and shielded to avoid excessive repulsion at short distances. For a more detailed description of the ReaxFF method, see the following references by van Duin et al.,^{S2} van Duin and Larter,^{S3} and Chenoweth et al.^{S4}

In this work, the ReaxFF for the ternary Ru-N-H system was developed. The force field parameters were optimized against first-principles data presented in the training set using a single parameter-based parabolic extrapolation method. The optimized parameters were the atom parameters for Ru; the bond parameters for Ru-Ru, Ru-N and Ru-H; and the off-diagonal parameters for Ru-N and Ru-H. The ReaxFF parameters for the binary N-H

systems were taken from a previous report.^{S5} The training set was a collection of results (energies, geometries, atomic charges, etc.) obtained from first-principles calculations that consists of equations of states (EOSs) for various Ru crystals, formation energies of Ru surfaces, various reaction pathways on Ru surfaces (adsorption and diffusion behaviors of N and H atoms, energy barriers for N₂ dissociation and NH₃ association, and so on), and bond dissociation behaviors of Ru-N and Ru-H in cluster models.

For first-principles calculations in periodic systems, the Vienna Ab-initio Simulation Package (VASP)^{S6} was used with an energy cutoff of 500 eV and the Perdew-Burke-Ernzerhof (PBE)^{S7} exchange and correlation functional. The project-augmented-wave method was adopted to describe the core electrons, and the k-points of 9×9×6 were used. The data points of the EOS were chosen to give adequate descriptions of the volume-energy relations for three polymorphs (hcp, fcc and bcc) of Ru. For each crystal, approximately 10 data points were considered, with an increment of ~2% between points. In addition, in searching the transition states (TSs) for the diffusion of N and H atoms, as well as the N₂ dissociation and NH₃ association reactions, nudged-elastic band (NEB)^{S8} calculations were also performed.

Figure S1 shows the EOSs of the three Ru crystals (fcc, bcc, and hcp) predicted by ReaxFF and first-principles calculations (DFT, density functional theory), and the optimized lattice parameters for each crystal are summarized in Table S1. Moreover, the cohesive energy of the hcp Ru crystal and the surface energies of various surfaces are summarized in Table S2.

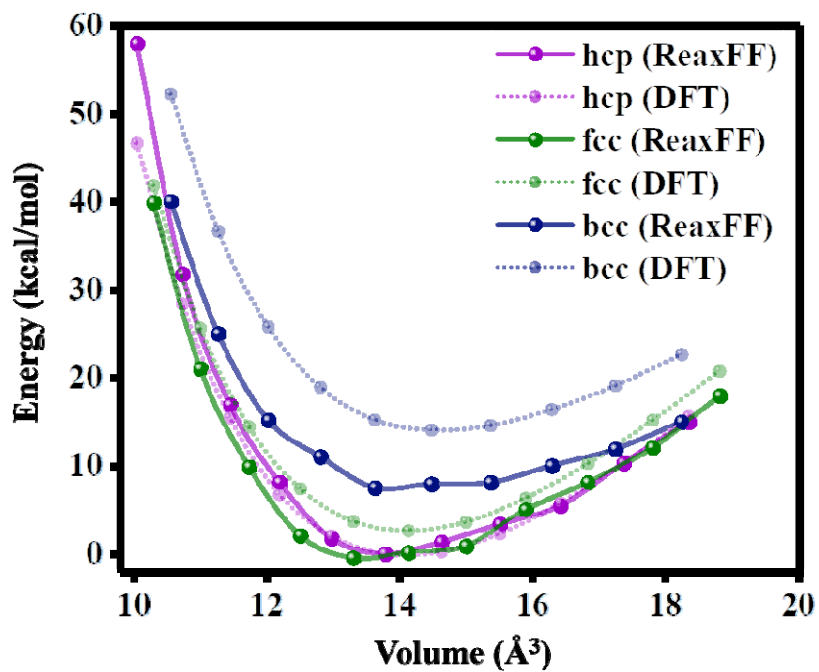


Figure S1. Comparison between DFT (dotted) and ReaxFF (solid) for the EOS of Ru crystals.

Table S1. Comparison between DFT (dotted) and ReaxFF (solid) for the lattice parameters for Ru crystals.

	Lattice parameters (Å)			
	HCP (<i>a</i>)	HCP (<i>c</i>)	FCC (<i>a</i>)	BCC (<i>a</i>)
ReaxFF	2.73	4.41	2.73	5.05
DFT	2.64	4.27	2.64	4.89

Table S2. Comparisons between DFT and ReaxFF for a cohesive energy of the hcp Ru crystal, and various Ru surfaces.

	Cohesive energy (kcal/mol)	Surface formation energy (J/m ²)			
		(100)	(111)	(110)	(0001)
ReaxFF	145.70	3.44	3.40	3.01	1.52
DFT	146.60	2.98	3.02	3.08	2.37

To calculate the binding energies of N and H atoms on the Ru(0001) surface, DFT calculations were carried out, and the results were used in developing the ReaxFF parameters. The preferential adsorption sites of the atoms predicted in our DFT calculations are in good agreement with previous reports.^{S9-S12} In other words, both the N and H atoms preferentially locate at three-fold hollow sites; however, the N atom prefers the hcp site, while the H atom prefers the fcc site. Here, when performing the DFT calculations, the Ru(0001) surface was modeled as a periodic slab with four Ru layers and a vacuum of 10 Å between slabs. Figures S2 and S3 show comparisons of the DFT and ReaxFF adsorption energy profiles of N and H atoms on the Ru(0001) surface. The most stable adsorption site for N atoms on the surface is the position that is separated by 1.047 Å from the top layer of the Ru hcp site (Figure S2). Indeed, according to a low-energy electron diffraction experiment,^{S10} the N atom preferentially locates at the Ru hcp site 1.05±0.05 Å from the Ru surface. On the other hand, the H atom is adsorbed at a distance of 1.068 Å from the top layer of the Ru fcc site (Figure S3). The developed ReaxFF reproduces the DFT energy profiles well

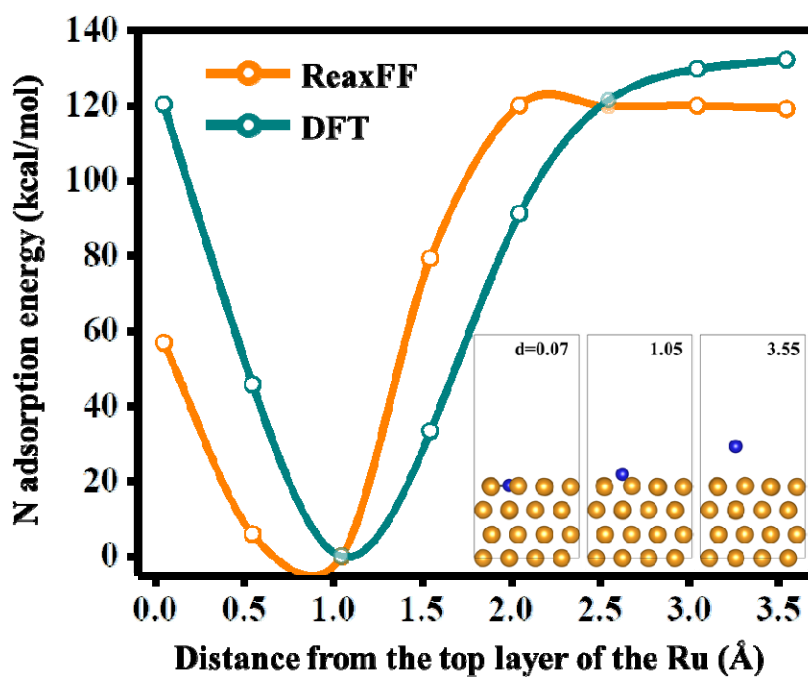


Figure S2. Adsorption energy profile of a N atom on the Ru(0001) surface.

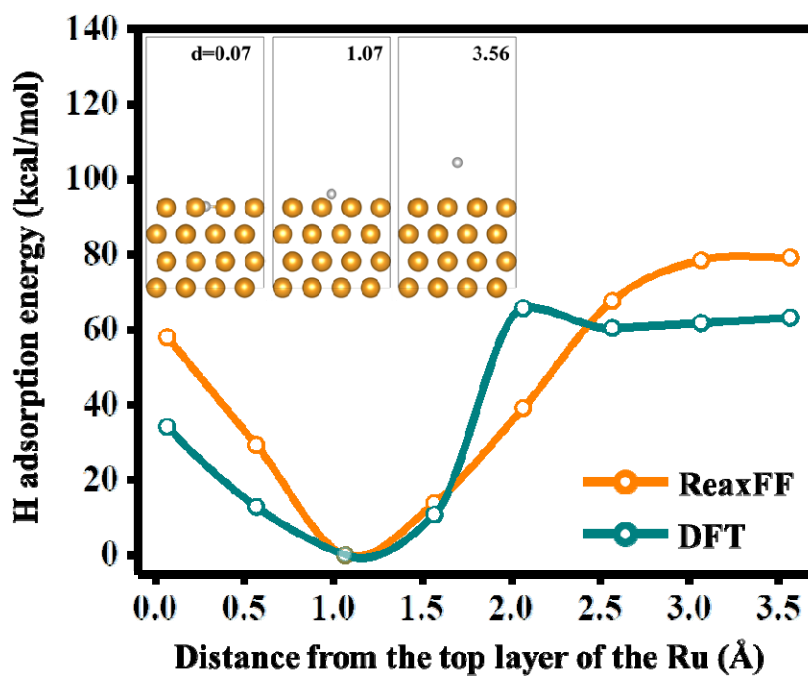


Figure S3. Adsorption energy profile of a H atom on the Ru(0001) surface.

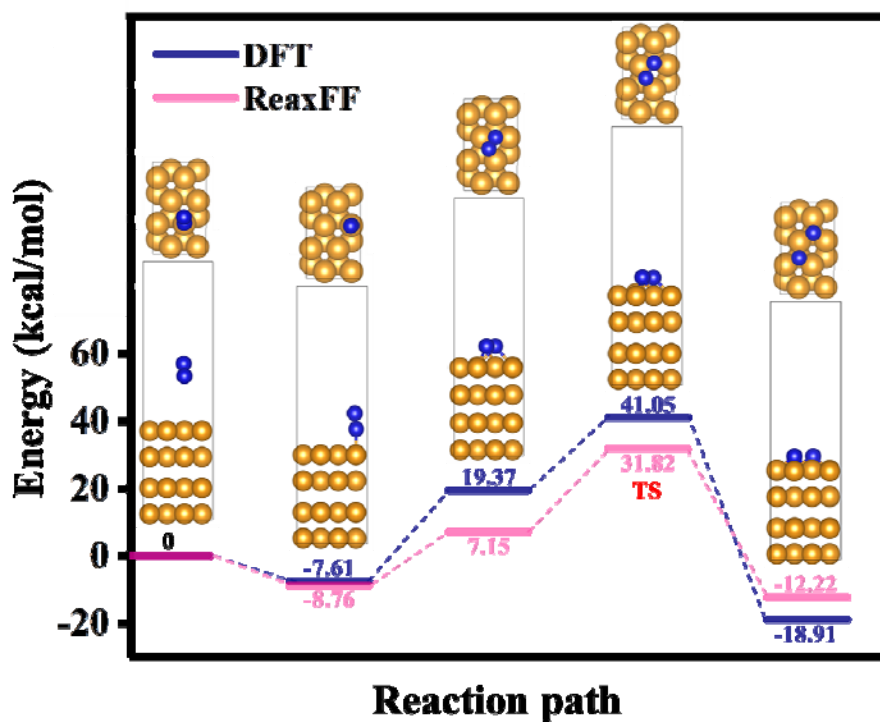


Figure S4. Potential energy diagram for N₂ dissociation on the Ru(0001) surface (DFT: navy, ReaxFF: pink). Here, the five structures correspond to N₂ gas phase, N₂ adsorption (vertical configuration) on the surface, metastable adsorption (parallel configuration), TS structure, and dissociated N structure. Color codes for atoms are blue = N and gold = Ru.

Figure S4 shows the potential energy diagram for the N₂ dissociation pathway on the terrace surface of Ru(0001). We can clearly see that the developed ReaxFF reproduces the DFT energy profile well. The energy barrier for N₂ dissociation is found to be 48.6 kcal/mol by DFT and 40.6 kcal/mol by the developed ReaxFF. In addition, the energy difference between the associated adsorption of nitrogen and the dissociated adsorption is exothermic by 11.30 kcal/mol (DFT) and 3.46 kcal/mol (ReaxFF). For the step site (Figure S5), our ReaxFF reveals the energy barrier of 11.0 kcal/mol, which is very similar to the reported DFT value

(9.2 kcal/mol)^{S14}.

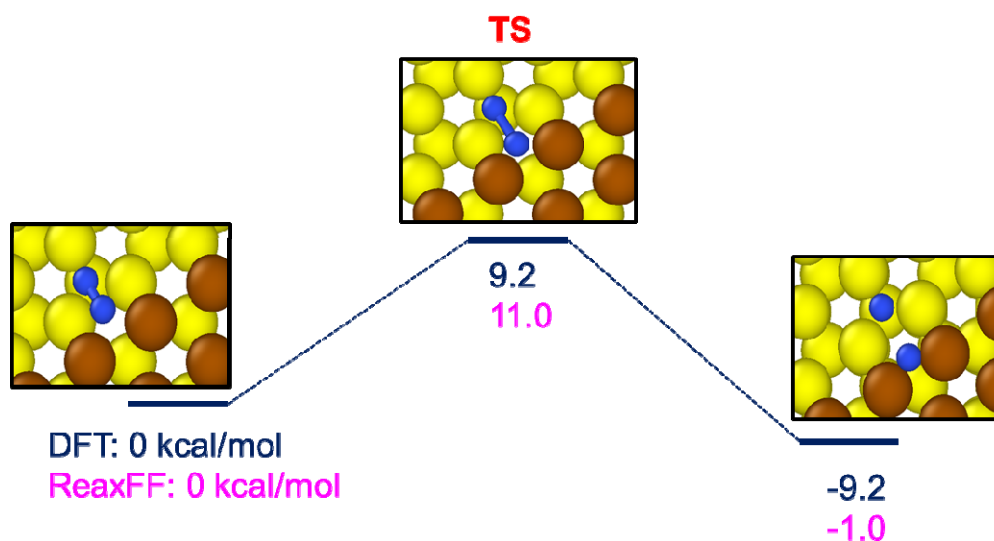


Figure S5. Calculated energy diagram for N₂ dissociation over the stepped site of Ru(0001). Here, black and pink values correspond to the reported DFT (Ref. S14) and the ReaxFF, respectively. And color codes of atoms are blue = N, yellow = Ru on the lower step, and brown = Ru on the upper step.

Figure S6 shows the migration energy barriers of H and N atoms on the Ru(0001) surface, obtained from NEB calculations. As already mentioned, the H atom is likely to locate on the three-fold fcc site, while the N atom locates on the three-fold hcp site. For both H and N migration, two paths were considered. For H diffusion, the first path (**A**) is the migration from the fcc site to the hcp site, and the second path (**B**) is from the fcc site to another fcc site. In addition, for N diffusion, the first path (**A**) is from the hcp site to the fcc site, and the second path (**B**) is from the hcp site to another hcp site. Although ReaxFF overestimates the migration energy barriers in comparison to DFT, it provides similar trends as DFT.

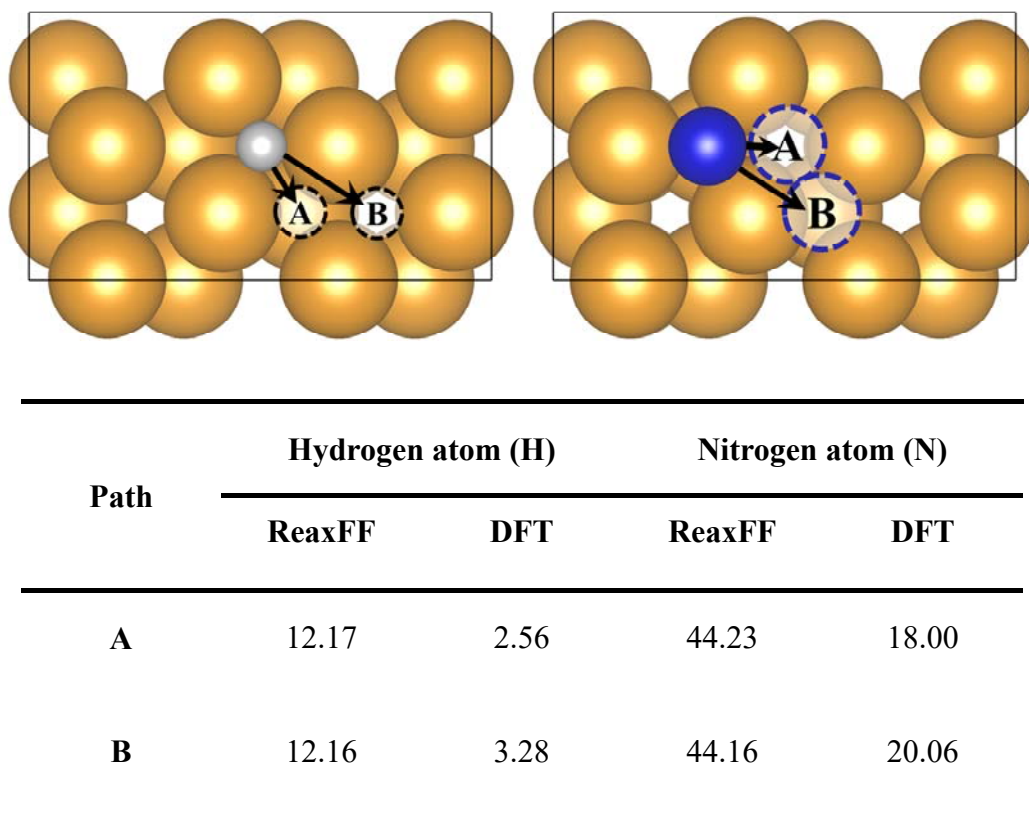


Figure S6. Migration energy barrier (units: kcal/mol) of H and N atoms on the Ru(0001) surface.

The process of NH_3 synthesis from dissociated N and H atoms on a Ru(0001) surface is modeled in Figure S7. As already mentioned, the H atom preferentially locates at the fcc site, while the N atom locates at the hcp site. As the first step for NH_3 synthesis, the H atom diffuses to the hcp site occupied by the N atom, and then, *NH is formed, as was suggested by Staufer et al.^{S13} According to Logadottir and Norskov,^{S14} NH_2 locates at a two-fold bridge site, and the most favorable adsorption site for NH_3 is the top site, which is also observed in our DFT calculation (Figure S7). They reported that the electron-rich N atom binds to the Ru surface at the most electron-deficient site, i.e., the top site.^{S15} A comparison between the DFT

and ReaxFF results for NH₃ synthesis (shown in Figure S7) is summarized in Table S3.

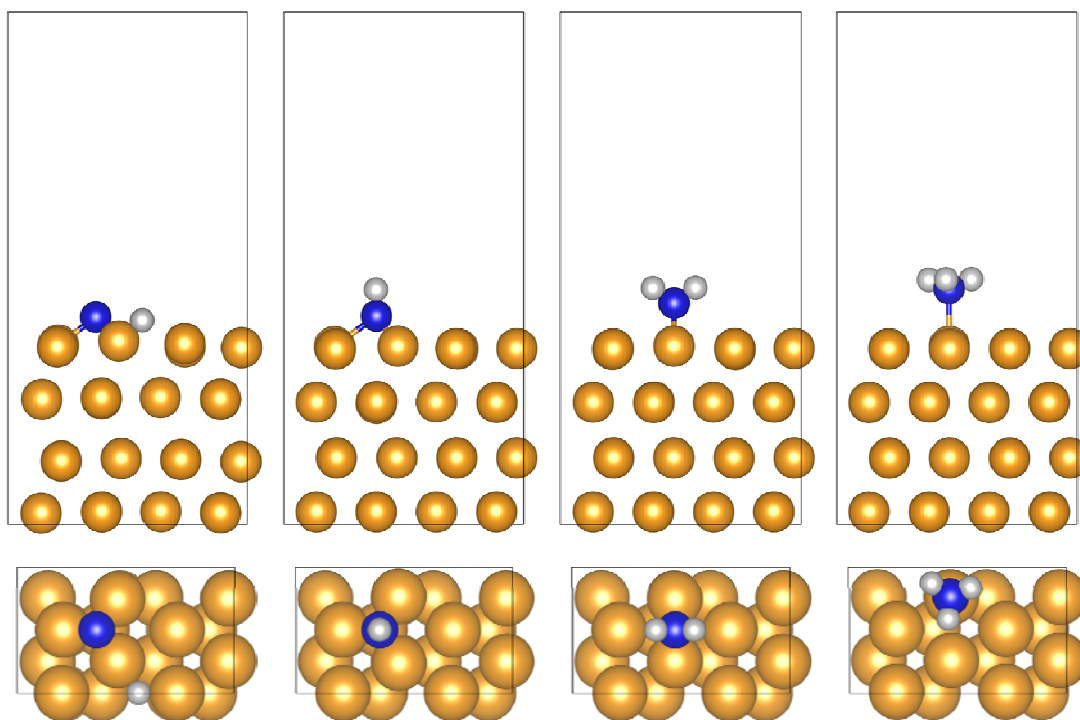


Figure S7. Snapshots of the $\ast\text{N}+\ast\text{H}$, $\ast\text{NH}$, $\ast\text{NH}_2$, and $\ast\text{NH}_3$ configurations on Ru(0001) during NH₃ synthesis. All of the snapshots correspond to optimized structures.

Table S3. Comparison between the DFT and ReaxFF energy barriers of several reaction pathways for NH₃ synthesis.

Reaction	Site	Energy barrier (kcal/mol)	
		ReaxFF	DFT
$\text{N}^\ast + \text{H}^\ast \rightarrow \text{NH}^\ast + \ast$	Hcp	52.60	24.40
$\text{NH}^\ast + \text{H}^\ast \rightarrow \text{NH}_2^\ast + \ast$	Bridge	28.78	29.98
$\text{NH}_2^\ast + \text{H}^\ast \rightarrow \text{NH}_3 + \ast$	Top	42.40	27.70

DFT calculations for cluster systems were performed using the Q-Chem software (version 4.1.0)^{S16} with the Becke three-parameter plus Lee-Yang-Parr (B3LYP) functional^{S17} and the Pople 6-311G** basis set^{S18}. These cluster calculations were mainly considered in developing the Ru-N and Ru-H bond terms in ReaxFF. Figure S8 shows the energy profile of bond dissociation between the Ru and N atoms in the $\text{Ru}(\text{NH}_3)_5(\text{N}_2)_1$ cluster while the distance between Ru and N is changed from 1.2 to 5 Å. In addition, Figure S9 shows the energy profile for bond dissociation between the Ru and H atoms in the RuH_4 cluster while the bond distances between Ru and H are changed from 1.2 to 4.5 Å.

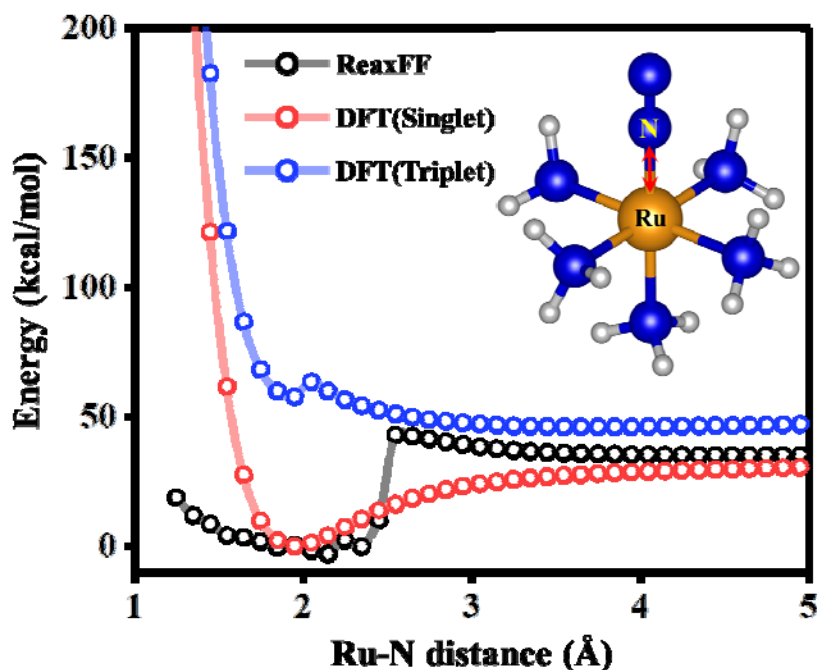


Figure S8. Energy profile for bond dissociation between the Ru and N atoms in the $\text{Ru}(\text{NH}_3)_5(\text{N}_2)_1$ cluster.

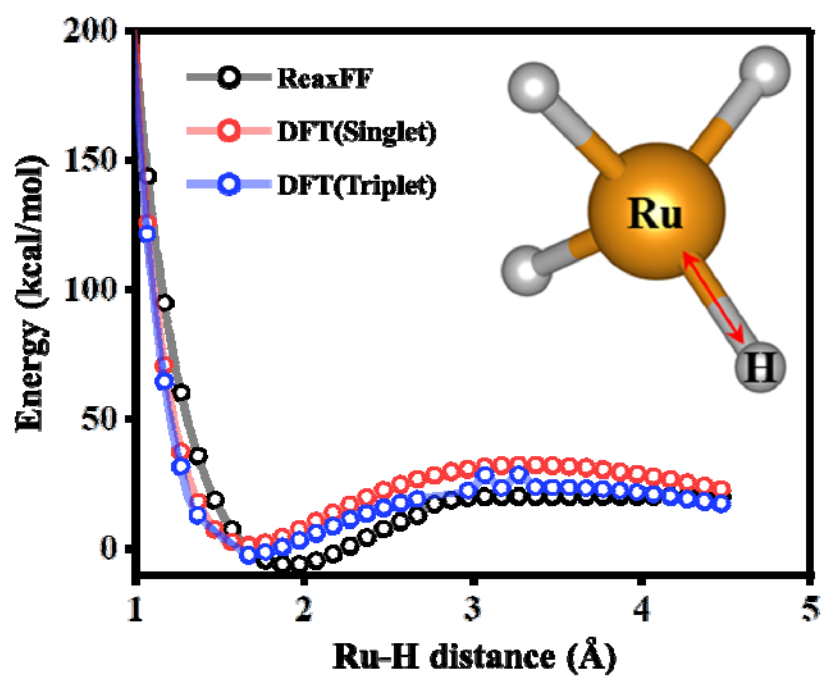


Figure S9. Energy profile for bond dissociation between the Ru and H atoms in the RuH₄ cluster.

Table S4. The developed ReaxFF for the Ru-N-H system

39	! Number of general parameters
50.0000	!Overcoordination parameter
9.5469	!Overcoordination parameter
1.6725	!Valency angle conjugation parameter
1.7224	!Triple bond stabilisation parameter
6.8702	!Triple bond stabilisation parameter
60.4850	!C2-correction
1.0588	!Undercoordination parameter
4.6000	!Triple bond stabilisation parameter
12.1176	!Undercoordination parameter
13.3056	!Undercoordination parameter
-70.5044	!Triple bond stabilization energy
0.0000	!Lower Taper-radius
10.0000	!Upper Taper-radius
2.8793	!Not used
33.8667	!Valency undercoordination
6.0891	!Valency angle/lone pair parameter
1.0563	!Valency angle
2.0384	!Valency angle parameter
6.1431	!Not used
6.9290	!Double bond/angle parameter
0.3989	!Double bond/angle parameter: overcoord
3.9954	!Double bond/angle parameter: overcoord
-2.4837	!Not used
5.7796	!Torsion/BO parameter
10.0000	!Torsion overcoordination
1.9487	!Torsion overcoordination
-1.2327	!Conjugation 0 (not used)
2.1645	!Conjugation
1.5591	!vdWaals shielding
0.1000	!Cutoff for bond order (*100)
1.7602	!Valency angle conjugation parameter
0.6991	!Overcoordination parameter
50.0000	!Overcoordination parameter
1.8512	!Valency/lone pair parameter
0.5000	!Not used
20.0000	!Not used
5.0000	!Molecular energy (not used)
0.0000	!Molecular energy (not used)
0.7903	!Valency angle conjugation parameter
3	! Nr of atoms; cov.r; valency;a.m;Rvdw;Evdw;gammaEEM;cov.r2;#
	alfa;gammavdW;valency;Eunder;Eover;chiEEM;etaEEM;n.u.
	cov r3;Elp;Heat inc.;n.u.;n.u.;n.u.;n.u.

```

ov/un;val1;n.u.;val3,vval4
H   0.8930  1.0000  1.0080  1.3550  0.0930  0.8203 -0.1000  1.0000
     8.2230 33.2894  1.0000  0.0000 121.1250  3.7248  9.6093  1.0000
    -0.1000  0.0000 55.1878  3.0408  2.4197  0.0003  1.0698  0.0000
   -19.4571  4.2733  1.0338  1.0000  2.8793  0.0000  0.0000  0.0000
N   1.2333  3.0000 14.0000  1.9324  0.1376  0.7921  1.1748  5.0000
    10.0667  7.8431  4.0000 32.2482 100.0000  7.5795  6.3952  2.0000
     1.0433 27.4290 119.9837  1.9457  4.2874  3.4869  0.9745  0.0000
    -4.3875  2.6192  1.0183  4.0000  2.8793  0.0000  0.0000  0.0000
Ru  2.3261  4.0000 101.0700  2.0925  0.3287  0.3000  0.2553  8.0000
    12.5211  4.7611  4.0000  0.0036 -0.0021  4.6329  6.0088  0.0000
     0.1000  0.0000 92.5072 66.6047 14.4716  0.1542  0.8563  0.0000
    -7.4697  2.4327  1.0338  8.0000  2.5791  0.0000  0.0000  0.0000
6   ! Nr of bonds; Edis1;LPpen;n.u.;pbe1;pbo5;13corr;pbo6
      pbe2;pbo3;pbo4;Etrip;pbo1;pbo2;ovcorr
1  1 153.3934  0.0000  0.0000 -0.4600  0.0000  1.0000  6.0000  0.7300
     6.2500  1.0000  0.0000  1.0000 -0.0790  6.0552  0.0000  0.0000
2  2 157.9384 82.5526 152.5336  0.4010 -0.1034  1.0000 12.4261  0.5828
     0.1578 -0.1509 11.9186  1.0000 -0.0861  5.4271  1.0000  0.0000
1  2 185.3171  0.0000  0.0000 -0.3689  0.0000  1.0000  6.0000  0.2854
     7.6517  1.0000  0.0000  1.0000 -0.0408  6.0255  0.0000  0.0000
1  3  50.9321  0.0000  0.0000 -0.7608  0.0000  1.0000  6.0000  0.0828
     1.9610  1.0000  0.0000  1.0000 -0.0954  6.4957 -0.0007  0.0000
2  3 149.0897 17.8495  0.0000 -0.5386 -0.4000  1.0000 25.000  0.0500
     0.1086 -0.2500 15.0000  1.0000 -0.1382  6.9697  0.9753  0.0000
3  3  79.0281  0.0000  0.0000  0.1501 -0.4000  1.0000 25.000  0.6146
     1.7906 -0.2500 15.0000  1.0000 -0.0809  4.9699  1.0000  0.0000
4   ! Nr of off-diagonal terms; Ediss;Ro;gamma;rsigma;rpi;rpi2
1  2  0.0687  1.5130 10.0094  0.9412 -1.0000 -1.0000
1  3  0.0696  1.7111 11.4650  1.8927 -1.0000 -1.0000
2  3  0.2139  2.3139  9.6078  1.6267 -1.0000 -1.0000
3  3  0.2780  1.8618 12.4800  1.6109  1.5301  1.2335
10  ! Nr of angles;at1;at2;at3;Thetao,o;ka;kb;pv1;pv2
1  1 1  0.0000 27.9213  5.8635  0.0000  0.0000  0.0000  1.0400
2  2 2 75.0538 14.8267  5.2794  0.0000  3.0000  0.0000  1.2127
1  2 2 83.0104 43.4766  1.5328  0.0000  0.3481  0.0000  1.5443
1  2 1 79.6336 17.7917  3.7832  0.0000  0.0222  0.0000  2.0238
2  1 2  0.0000  0.0019  6.0000  0.0000  0.0000  0.0000  1.0400
1  1 2  0.0000  0.0019  6.0000  0.0000  0.0000  0.0000  1.0400
2  3 2 79.1495 20.0000  4.0000  0.0000  1.0000  0.0000  1.0000
3  2 3 88.6173 20.0000  4.0000  0.0000  1.0000  0.0000  1.0000
1  3 1 82.6907  6.2388  3.3599  0.0000  1.0000  0.0000  1.6681
3  1 3 88.6095 18.0429  4.0000  0.0000  1.0000  0.0000  4.0000
3   ! Nr of torsions;at1;at2;at3;at4;;V1;V2;V3;V2(BO);vconj;n.u;n
0  1 1 0  0.0000  0.0000  0.0000  0.0000  0.0000  0.0000  0.0000

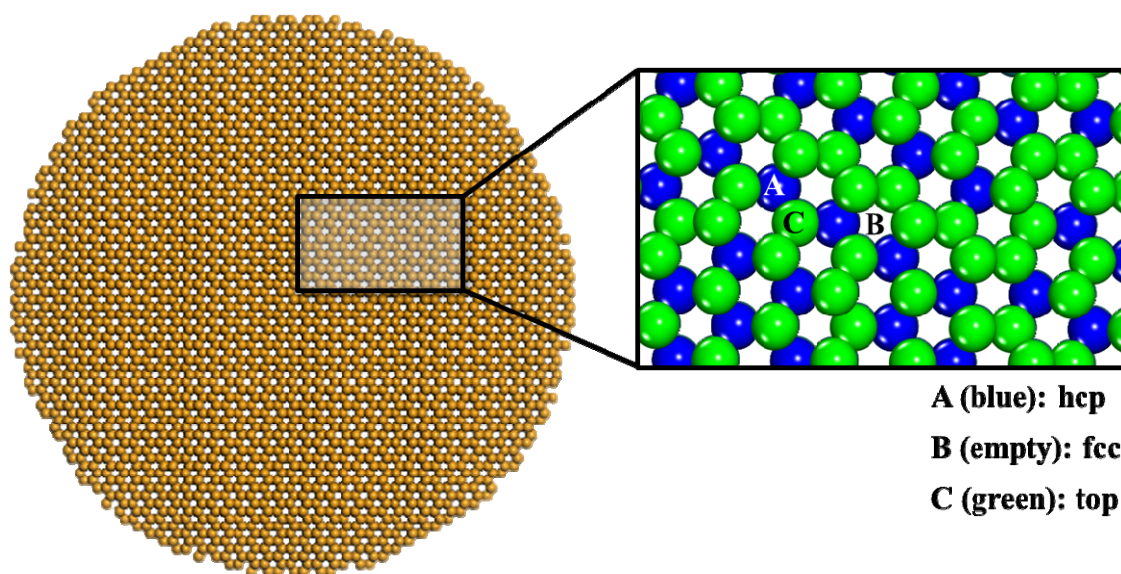
```

0	1	2	0	-1.5000	0.1032	0.0100	-5.0965	0.0000	0.0000	0.0000
0	2	2	0	0.7265	44.3155	1.0000	-4.4046	-2.0000	0.0000	0.0000
1	! Nr of hydrogen bonds;at1;at2;at3;Rhb;Dehb;vhb1									
2	1	2		1.9336	-5.8831	1.4500	19.5000			

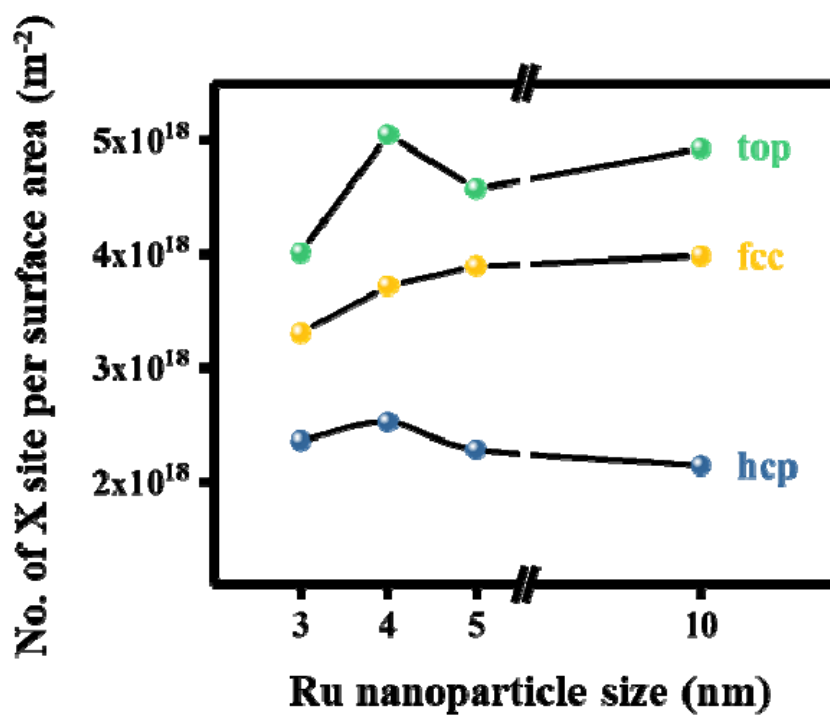
S2. Structural information of the Ru NPs considered in this work

Table S5. Number of atoms and surface area for Ru NPs with diameters of 3, 4, 5, and 10 nm.

	3 nm	4 nm	5 nm	10 nm
Number of atom	1,050	2,488	4,842	38,570
Number of surface atom	522	980	1,548	6,536
Surface area (m²)	3.39 x 10 ⁻¹⁷	6.02 x 10 ⁻¹⁷	9.45 x 10 ⁻¹⁷	3.74 x 10 ⁻¹⁶
Surface area (m²/g)	192.30	144.21	116.25	57.69
Surface area (m²/surface atom)	6.49 x 10 ⁻²⁰	6.15 x 10 ⁻²⁰	6.10 x 10 ⁻²⁰	5.72 x 10 ⁻²⁰



(a)



(b)

Figure S10. (a) The hcp, fcc, and top sites on the Ru NP surface and (b) number per surface area of hcp, fcc, and top sites on the 3, 4, 5, and 10 nm Ru NP surfaces.

S3. Additional ReaxFF results

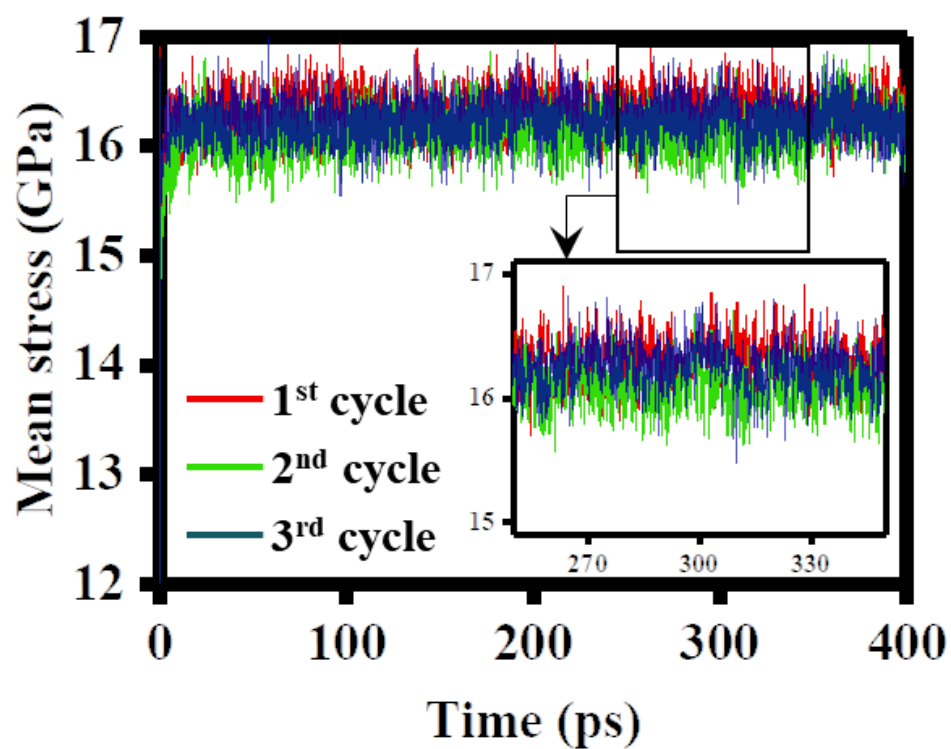


Figure S11. The mean von Mises stress for the 3 nm Ru NP as a function of the 1st, 2nd, and 3rd NH₃ synthesis cycle.

In this work, we used a high temperature such as 1,500 K to accelerate the chemical reactions between the Ru NPs and N₂/H₂ gases, although the conventional Haber-Bosh process was usually performed in the temperature range of 673~773 K. Thus, to justify the use of the 1,500 K, we additionally performed MD simulations for N₂ dissociation on the 4 nm Ru NP at various temperatures (700, 900, 1100, and 1300 K), as shown in Figure S12.

For N₂ dissociation, the reaction rate at a given temperature can be expressed with the following equation:

$$[N^*] = [N_2]e^{-kt} \quad (S2)$$

where [N₂] and [N*] are numbers of N₂ molecules in the initial system and the dissociated nitrogen atom at a given time t , respectively, and k is a reaction constant.

With the Eq. (6), we fitted to the MD simulation results in Figure S12 and obtained k at each temperature, which is shown in Figure S13. And then, by the Arrhenius-type equation, we obtained an energy barrier (17.1 kcal/mol) for the N₂ dissociation on the 4 nm Ru NP. According to a reported DFT calculation,^{S14} energy barriers for N₂ dissociation over Ru surfaces are 43.8 kcal/mol (our DFT calculation: 48.6 kcal/mol) over terrace surfaces and 9.2 kcal/mol over step surfaces. Because the 4 nm Ru NP considered in our MD simulation has both of the terrace and step, it can be expected that an energy barrier over the NP surfaces is between 9.2 and 43.8 kcal/mol. Indeed, our MD simulations performed at various temperatures reveal the energy barrier of 17.1 kcal/mol. We believe that this can justify the use of 1,500 K in this work.

In addition, according to Ref. S14, an energy barrier for H₂ dissociation over the Ru surfaces is almost zero for both of the terrace and step sites. Indeed, our ReaxFF-MD simulation also shows a zero energy barrier for H₂ dissociation (Figure S14b).

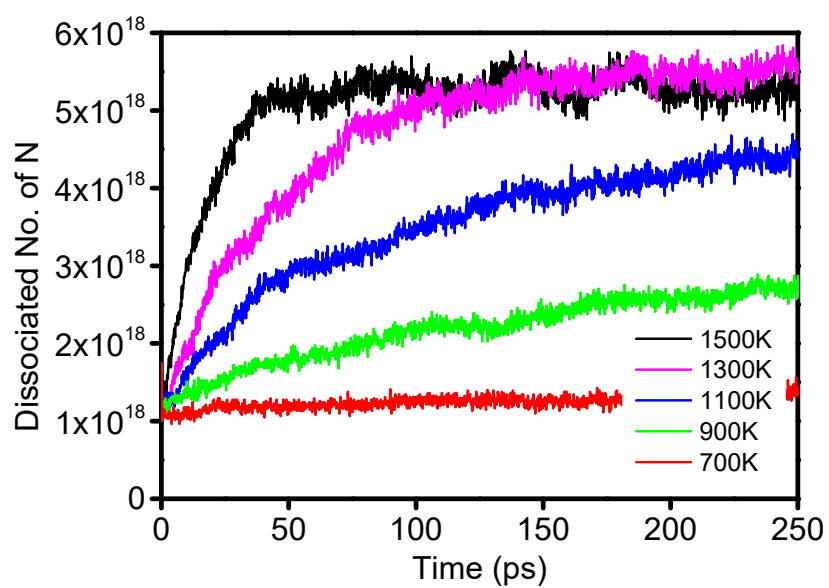


Figure S12. Number (No.) of dissociated N on the 4 nm Ru NP.

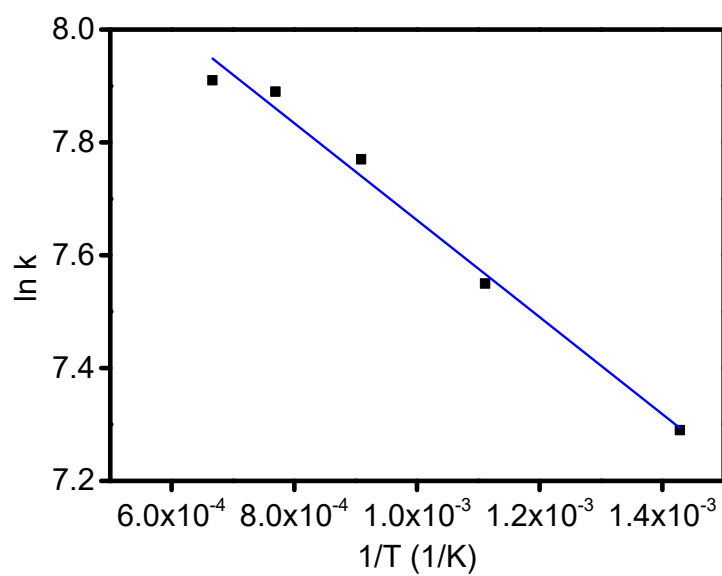


Figure S13. Rate of N₂ dissociation as a function of temperature.

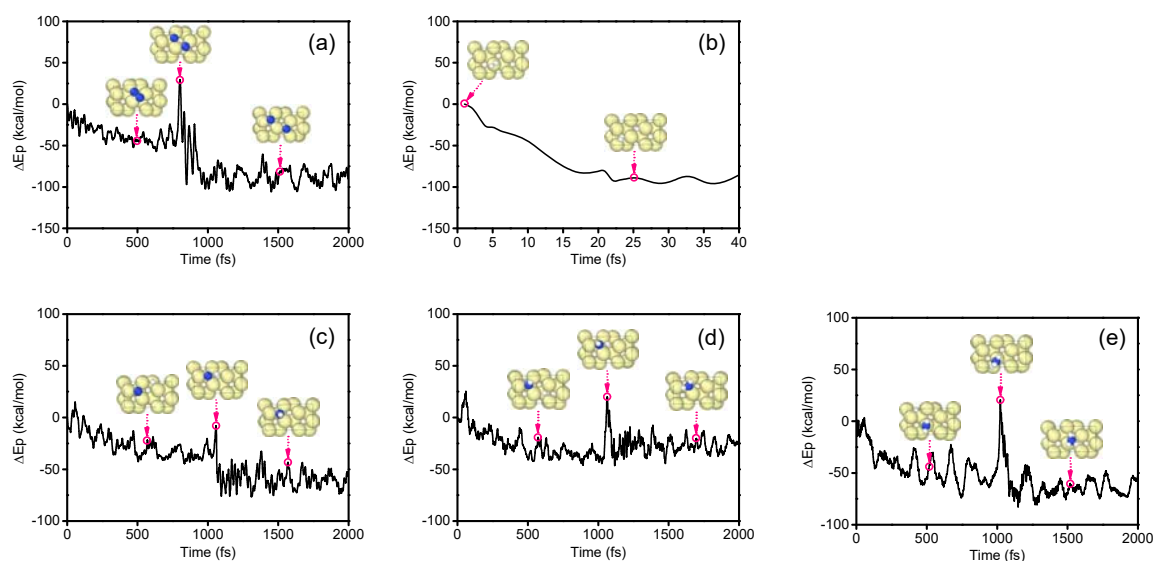


Figure S14. Constrained MD simulations for each elementary steps of NH_3 synthesis on Ru(0001) surface at 700 K. (a) $\text{N}_2 + 2^* \rightarrow 2\text{N}^*$, (b) $\text{H}_2 + 2^* \rightarrow 2\text{H}^*$, (c) $\text{N}^* + \text{H}^* \rightarrow \text{NH}^* + ^*$, (d) $\text{NH}^* + \text{H}^* \rightarrow \text{NH}_2^* + ^*$, and (e) $\text{NH}_2^* + \text{H}^* \rightarrow \text{NH}_3^* + ^*$.

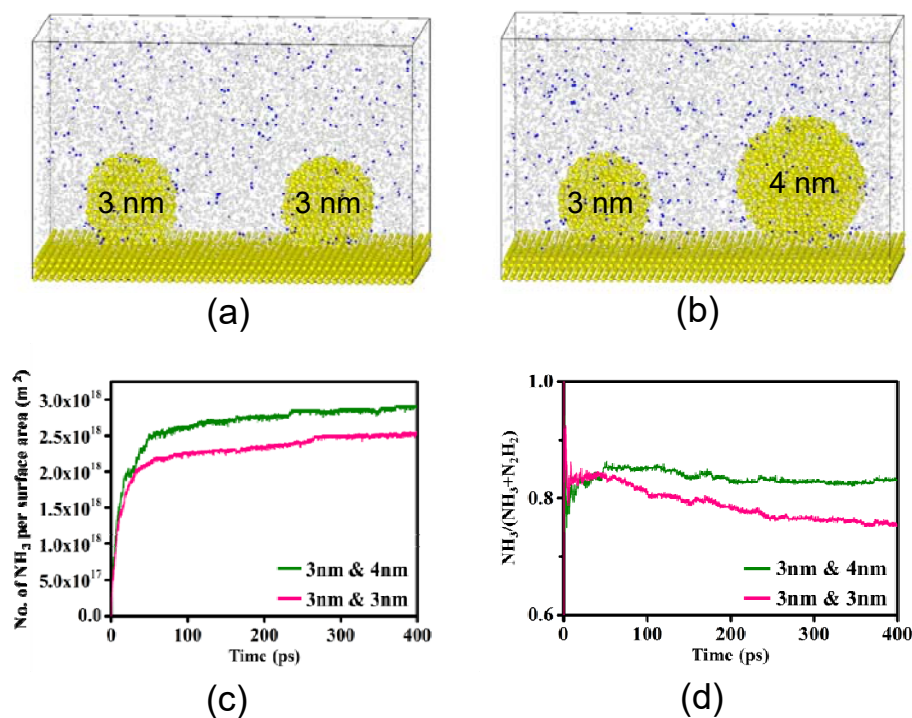


Figure S15. (a, b) MD snapshots for the systems including two 3 nm Ru NPs (a) and including the 3 and 4 nm NPs (b) after H_2 purging, leading to NH_3 generation. (c) numbers of generated NH_3 (activity) for the (a) and (b) simulation models. (d) $\text{NH}_3/(\text{N}_2\text{H}_2 + \text{NH}_3)$ (selectivity) for the (a) and (b).

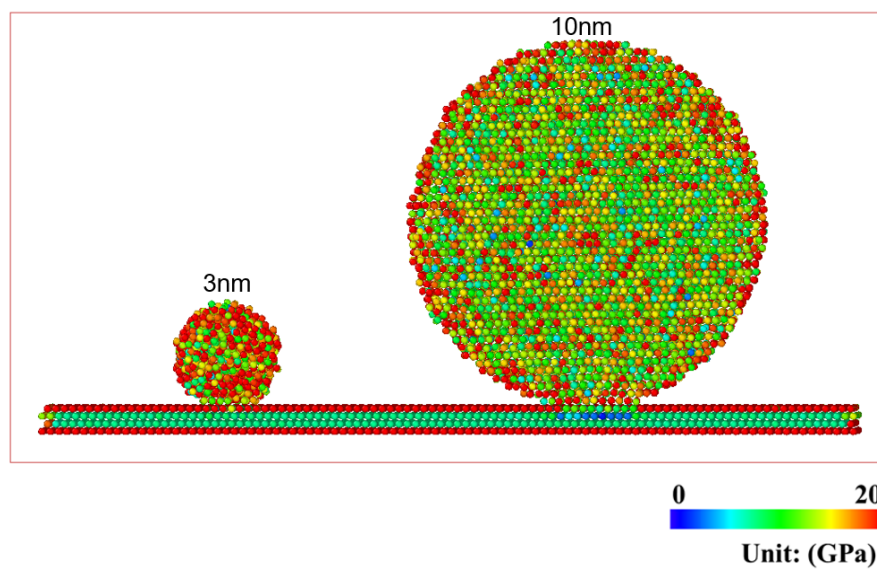


Figure S16. Distribution of the von Mises stresses on the surfaces and cross sections of the 3 nm and 10 nm Ru NPs obtained after the N₂ dissociation process of 100 ps.

References

- (S1) Mortier, W. J.; Ghosh, S. K.; Shankar, S., Electronegativity Equalization Method For the Calculation of Atomic Charges in Molecules. *Journal of the American Chemical Society* **1986**, *108* (15), 4315-4320.
- (S2) van Duin, A. C. T.; Dasgupta, S.; Lorant, F.; Goddard, W. A., ReaxFF: A Reactive Force Field for Hydrocarbons. *J. Phys. Chem. A* **2001**, *105* (41), 9396-9409.
- (S3) van Duin, A. C. T.; Larter, S. R., Molecular Dynamics Investigation into the Adsorption of Organic Compounds on Kaolinite Surfaces. *Organic Geochemistry* **2001**, *32* (1), 143-150.
- (S4) Chenoweth, K.; van Duin, A. C. T.; Goddard, W. A., ReaxFF Reactive Force Field for Molecular Dynamics Simulations of Hydrocarbon Oxidation. *J. Phys. Chem. A* **2008**, *112* (5), 1040-1053.
- (S5) Kamat, A. M.; van Duin, A. C. T.; Yakovlev, A., Molecular Dynamics Simulations of Laser-Induced Incandescence of Soot Using an Extended ReaxFF Reactive Force Field. *J. Phys. Chem. A* **2010**, *114* (48), 12561-12572.
- (S6) Kresse, G.; Furthmüller, J., Efficiency of Ab-initio Total Energy Calculations for Metals and Semiconductors Using a Plane-wave Basis Set. *Computational Materials Science* **1996**, *6* (1), 15-50.
- (S7) Perdew, J. P.; Burke, K.; Ernzerhof, M., Generalized Gradient Approximation Made Simple. *Physical Review Letters* **1996**, *77* (18), 3865-3868.
- (S8) Henkelman, G.; Uberuaga, B. P.; Jonsson, H., A Climbing Image Nudged Elastic Band Method for Finding Saddle Points and Minimum Energy Paths. *Journal of Chemical Physics* **2000**, *113* (22), 9901-9904.
- (S9) Jacobi, K.; Dietrich, H.; Ertl, G., Nitrogen Chemistry on Ruthenium Single-Crystal Surfaces. *Applied Surface Science* **1997**, *121*, 558-561.
- (S10) Schwegmann, S.; Seitsonen, A. P.; Dietrich, H.; Bludau, H.; Over, H.; Jacobi, K.; Ertl, G., The Adsorption of Atomic Nitrogen on Ru(0001): Geometry and Energetics. *Chemical Physics Letters* **1997**, *264* (6), 680-686.
- (S11) Shi, H.; Jacobi, K., Hydrogen Vibrations on the Ru(001) Surface Revisited. *Surface Science* **1994**, *313* (3), 289-294.
- (S12) Lindroos, M.; Pfnur, H.; Feulner, P.; Menzel, D., A Study of the Adsorption Sites of Hydrogen on Ru(001) at Saturation Coverage by Electron Reflection. *Surface Science* **1987**, *180* (1), 237-251.
- (S13) Staufer, M.; Neyman, K. M.; Jakob, P.; Nasluzov, V. A.; Menzel, D.; Rösch, N., Density Functional and Infrared Spectroscopy Studies of Bonding and Vibrations of NH Species Adsorbed on the Ru(001) Surface: A Reassignment of the Bending Mode Band. *Surface Science* **1996**, *369* (1), 300-312.
- (S14) Logadottir, A.; Norskov, J. K., Ammonia Synthesis over a Ru(0001) Surface Studied by Density Functional Calculations. *Journal of Catalysis* **2003**, *220* (2), 273-279.
- (S15) Norskov, J. K., Electronic Factors in Catalysis. *Prog. Surf. Sci.* **1991**, *38* (2), 103-144.
- (S16) Kong, J.; White, C. A.; Krylov, A. I.; Sherrill, D.; Adamson, R. D.; Furlani, T. R.; Lee, M. S.; Lee, A. M.; Gwaltney, S. R.; Adams, T. R.; Ochsenfeld, C.; Gilbert, A. T. B.; Kedziora, G. S.; Rassolov, V. A.; Maurice, D. R.; Nair, N.; Shao, Y. H.; Besley, N. A.; Maslen, P. E.; Dombroski, J. P.; Daschel, H.; Zhang, W. M.; Korambath, P. P.; Baker, J. J.

Byrd, E. F. C.; Van Voorhis, T.; Oumi, M.; Hirata, S.; Hsu, C. P.; Ishikawa, N.; Florian, J.; Warshel, A.; Johnson, B. G.; Gill, P. M. W.; Head-Gordon, M.; Pople, J. A., Q-chem 2.0: A High-Performance Ab Initio Electronic Structure Program Package. *Journal of Computational Chemistry* **2000**, 21 (16), 1532-1548.

(S17) Becke, A. D., Density-Functional Thermochemistry .3. The Role of Exact Exchange. *Journal of Chemical Physics* **1993**, 98 (7), 5648-5652.

(S18) Krishnan, R.; Binkley, J. S.; Seeger, R.; Pople, J. A., Self-Consistent Molecular Orbital Methods. XX. A Basis Set for Correlated Wave Functions. *Journal of Chemical Physics* **1980**, 72 (1), 650-654.